https://jksus.org

Journal of King Saud University – Science

2025 37 (2) 2592024

Research Article

Probing the solvent effects and protonation sites of 1-phenyl-4-(phenyldiazenyl)-1H-pyrazol-5-amine (PDPA): DFT calculations meet pKa profiling

Zaki Safi[a], Nuha Wazzan[b,*]

[a]Department of Chemistry, Al Azhar University, Jamal Abdel Nasser, Gaza, 1277, Palestinian Territory, Occupied
[b]Department of Chemistry, Faculty of Science, King Abdulaziz University, P.O Box 42805, Jeddah 21589, Saudi Arabia

ARTICLE INFO

Keywords:
Gas-phase basicity (GB)
Intermolecular hydrogen bond (IMHB)
PDPA
Proton affinity (PA)
Quantum theory of atoms in molecules (QTAIM)

ABSTRACT

5-methyl-2-phenyl-4-(2-phenylhydrazono)-2,4-dihydro-3H-pyrazol-3-one (PDPA) was recently synthesized as a promising nuclear magnetic resonance (NMR) reference in studying the tautomeric structures of azo dyes. In this study, the interaction of PDPA derivatives with a single water molecule was studied using the density functional theory (DFT) method. The protonation reaction was proposed to identify the most basic center in the investigated species by computing the proton affinity (PA) and gas phase basicity (GB) values. The nature of the intermolecular hydrogen bond (IMHB) due to the interaction of the hydrogen atom of the water molecule and the nitrogen atom of the PDPA molecule was investigated using several aspects, including geometrical structures, quantum theory of atoms in molecules (QTAIM), natural bond orbital (NBO) analysis and the noncovalent interactions (NCIs) using the reduced density gradient (RDG) MAPS. Results revealed that the PDPA derivatives are medium potent and basic with average PA and GB values of 219.7 and 213.0 kcal/mol, respectively. The maximum PA and GB values of 228.5 and 221.7 were found for the PDPA-NH_2 derivative, respectively, while the smallest ones of 213.5 and 206.7 for the PDPA-CN derivative, reflecting the effect of the nature of the substituted group. Our results revealed that IMHB has moderate strength and is strongly dependent on the nature of the substituted group. The results of QTAIM indicated that the average IMHB strength is 5.0 kcal/mol and that between the water molecule and thiazolidine-2,4-dione and its derivatives is 4.8 kcal/mol. Moreover, NBO analysis showed that the average IMHB strength is 6.7 kcal/mol. Results also revealed that substitution of the electron donating groups strengthens the IMHB, while that of the electron withdrawing groups weakens it.

1. Introduction

Azo dyes, which constitute over 65% of the synthetic dyes, are a huge and significant type of dyes. These dyes are used in some foods, textiles, and leather articles (Correia *et al.*, 1994). Some examples include water-soluble azo dyes based on H-acid, J-acid, and γ-acid. Azo dyes have various biological applications in molecular data processing, such as in ion sensors and optical materials (Geng *et al.*, 2015). Although useful, azo dyes can impact the quality of ground water by blocking light transmission, affecting photosynthesis, and reducing dissolved oxygen in water (Meghwal *et al.*, 2020). Chemically, azo dyes consist of an aminobenzene group, including Ar-N=N-P(NH_2)-Ar, Ar-N-N=P(C=O)-Ar, and Ar-N=N-Ar, where Ar, P(C=O), P(NH_2) (Zollinger 2003). The nature of the substituted groups on the phenyl ring plays a vital role in the discrepancy of the chemical and physical properties (solubility or color) of the azo dyes (Cerezo *et al.*, 2015; Comez *et al.*, 2016).

Among the numerous molecular properties that can be calculated for the molecular compounds are proton affinity (PA) and gas-phase basicity (GB), which are associated with the protonation reaction. PA and GB represent the negative values of the change in enthalpy (ΔH) and Gibbs free energy (ΔG), respectively. Furthermore, PA and GB properties are very useful in the investigation of proton donor and acceptor position. The determination of PAs using experimental methods such as mass spectrometry (Valadbeigi and Farrokhpour, 2013), kinetic methods, calorimetry, ion cyclotron resonance (Blake *et al.*, 2009), and ion mobility spectrometry (Tabrizchi and Shooshtari, 2003) is often challenging (Dixon and Lias, 1987). The accuracy of the experimental PA and GB values, as well as the challenges, difficulties, and quantities of the available materials, leads to the use of computational methods as alternatives. Most studies used Density Functional Theory (DFT) methods to calculate PA and GB quantities, which tend to calculate these quantities as accurately as the high-level *ab-initio* methods such as MP2 and CCTD (Rebber *et al.*, 2006; Safi and Wazzan, 2021).

There are various types of noncovalent solute-solvent interactions (NCI), which cover the solvation progression of soluble molecules in media of interest. In particular, intermolecular forces, which can include hydrogen bonds and electrostatic interactions that lead to changes in the physiochemical nature of the azo dyes (Bani-Yaseen 2017). The interaction of water molecules can occur through implicit or explicit interaction. For explicit interactions, it is important to predict the most basic site that with the capability to interact with water molecules via intermolecular hydrogen bonds (IMHBs), which can occur by a protonation reaction (Safi and Omar 2014; Zhao and Zhang 2004).

IMHB is usually known as a weak non-covalent interaction involving a donor-acceptor pair. Quantum Theory of Atoms In Molecules (QTAIM) of Bader (Bader 1991) and Natural Bond Orbital (NBO) analysis

*Corresponding author
E-mail address: nwazzan@kau.edu.sa (N. Wazzan)

Received: 29 October, 2024 **Accepted:** 20 March, 2025 **Epub Ahead of Print:** 22 April, 2025 **Published:** 31 May 2025

DOI: 10.25259/JKSUS_259_2024

are repeatedly applied in the analysis of hydrogen bonds, including intermolecular and intramolecular H-bonds (Lamsabhi 2008; Safi 2016; Osman 2017; Bayoumy *et al.*, 2020; El-Sayed *et al.*, 2024). Analysis of the electron density at the bond critical point and its related topological parameters was compared with the results of traditional experiments such as X-ray measurements (Espinosa *et al.*, 1996; Espinosa *et al.*, 1998).

A recent study (Deneva *et al.*, 2019) synthesized and characterized two series of azo dyes derived from pyrazolamine and pyrazolone, which can be used as NMR reference in the study of the tautomerics of azo dyes. Of particular interest, 3-methyl-1-phenyl-4-(phenyldiazenyl)-1H-pyrazol-5-amine (PDPA) was chosen for this study (Scheme 1). As can be seen in Scheme 1, PDPA exhibits an exceptional characteristic based on the presence of a variety of functional groups. These functional groups can theoretically facilitate the noncovalent solute-solvent interactions with components present within its molecular environments. In the current study, the methyl group at position 5 of the pyrazol ring has been replaced by several groups with different natures, including H, NH_2, NO_2, CHO, Cl, F, and CN. We aim to provide insights into the explicit molecular solute-water interactions of PDPA using the DFT method. Protonation reaction was used to predict the most basic nitrogen atom that could explicitly interact with the water molecule. The nature of the intermolecular interactions between the PDPA derivatives and water molecule were analyzed and discussed in depth in terms of geometrical structures, QTAIM, NCI, and NBO analysis.

2. Computational details

Computational calculations and visualization of the investigated species were conducted using the Gaussian 09 software package (Gaussian09 2009) and Gaussview (Dennington *et al.*, 2016), respectively. Geometries of PDPA derivatives were optimized, followed by frequency calculations employing the DFT method with B3LYP (Becke 1996) functional and 6-311++g(d,p) level of theory in the gas phase. To improve the accuracy of the results, DFT-D3 and BJ-damping functional correction proposed by Grimme *et al* (S. Grimme 2010) was also used in geometry optimization. To achieve more reliable energy, single-point energy calculations were done using the B3LYP/6-311++g(3df,2p) level of theory. The selected level of theory was examined previously and found to compute accurate PA values (Nguyen and Chandra 1998; Safi 2016). The explicit solvent effect was computationally examined at the same level of theory by the complexation of the PDPA molecule and its derivatives with a single water molecule. The corresponding PA and GB of PDPA and its derivatives were calculated using the following expressions:

$$\left\{\begin{array}{c} PA = -\Delta H = \left[\Delta E_{elec} + \Delta ZPE + \Delta E_{vib} - \frac{5}{2}RT\right] \\ GB = -\Delta G = PA - T\Delta S \end{array}\right\} \quad (1)$$

Here, ΔE_{elec}, ΔZPE, and ΔE_{vib} represent, correspondingly, the differences between the total electronic energy, zero-point vibrational energy and temperature-dependent vibrational energy of reactants and products at T=298 K, between the neutral and protonated forms of PDPA derivatives. The (5/2)RT and $T\Delta S$ were taken as 1.48 and -6.28 kcal/mol, respectively (Safi and Omar 2014). A second-order perturbation method in the NBO framework (Reed *et al.*, 1988) was used to analyze

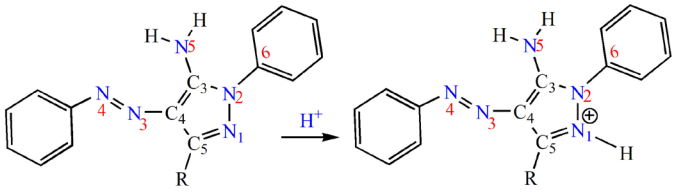

R = -H, -CH_3, -NH_2, -Cl, -F, -CN, -CHO, -NO_2

Scheme 1. Schematic representation of the studied PDPA molecule and its derivatives. PDPA: Poly (2,5-dialkyl-phenylene) amine.

the interactions between water molecules and PDPA derivatives. QTAIM analysis (Bader 1991) was performed using the Multiwfn software (Lu and Chen 2012). The NCI analysis, which is known as reduced density gradient (RDG), was performed using the independent gradient model (IGM) analysis based on promolecular density in the framework of Multiwfn sotware. RDG maps were visualized under VMD (Humphrey *et al.*, 1996) and Gnuplot (Kelley 2004-2021) programs.

3. Results and Discussion

The PDPA molecule has five nitrogen atoms, labeled N1, N2, N3, N4, and N5, which underwent protonation and consequently interacted with a water molecule during the solvation process via IMHB formation. A preliminary study based on pK_a calculation as implemented in the Marvin sketch program (Cherinka *et al.*, 2019) indicates that the N1 atom is the most preferable center for protonation; see Fig. SM1 of the supplementary materials. It is also important to mention that protonation of PDPA-F and PDPA-NO_2 has been excluded due to the reduction of the nitro group during the pK_a calculations and high electronegativity of the F atom. Furthermore, the % protonated form (%P) increases and decreases as the power of the EDG increases and EWG decreases, respectively.

3.1 Analysis PA and GB results

The calculated PA and GB values of the investigated species using the DFT method have been displayed in Table 1. The corresponding total energies, zero-point energy (ZPE), and the thermal corrections for energies, enthalpies, and Gibbs free energies (TCE, TCH, and TCG) have been collated in Table SM1 of the supplementary materials. Our preliminary DFT calculations for the parent PDPA-H molecule show that N2 and N5 are the least basic atoms with PA values of 189.2 and 189.2 kcal/mol, respectively; Whereas the competition between N1, N3, and N4 has been clearly observed. Based on these results, the PA and GB values of N1, N3, and N4 atoms have been considered in our discussion. It was found that N1 is more basic than N3 and N4. For the parent molecule, the PA and GB values of the N1 atom are higher than the corresponding ones for N3 and N4. The average PA and GB values of N1 and N2 atoms are 219.7 and 213.1 kcal/mol, respectively, compared with those of N3 (219.2 and 212.2 kcal/mol) and N4 (218.3 and 211.2 kcal/mol) atoms. The average PA and GB values indicate that all atoms have almost the same basicity, with the N1 atom being the most basic. These results agree with those obtained by pK_a calculation. These findings indicate that the PDPA molecule and its derivatives are moderate potent bases and their basicity is close to that of 5-metylhydantoin derivatives (PA=185-207 kcal/mol) (Safi and Frenking 2013), aniline (PA = 210 kcal/mol) (Jolly 1991), and triazepines derivatives (PA = 207 kcal/mol) (Safi and Lamsabhi 2007), with PA values of, 186.6-209.7 kcal/mol. It was also found that the basicity of the PDPA molecule is much higher than that of Helium (PA= 42.6 kcal/mol) and lower than that of methanide (PA = 416.8 kcal/mol) (Jolly 1991).

Table 1.
Gas phase proton affinity (PA) and basicity (GB) (at 298 K, in kcal/mol) for different PDPA derivatives.

PDPA derivatives	PA (kcal/mol)			GB (kcal/mol)		
	N1	N3	N4	N1	N3	N4
PDPA-H	223.5	220.0	218.6	217.1	212.7	211.6
PDPA-CH_3	226.5	222.4	220.0	220.5	215.0	212.6
PDPA-NH_2	228.5	219.1	225.2	221.7	212.0	218.0
PDPA-Cl	219.5	217.7	218.0	212.7	210.4	211.1
PDPA-F	216.5	216.0	216.8	209.7	209.4	209.5
PDPA-CHO	215.7	225.2	224.9	209.3	218.1	217.7
PDPA-CN	213.5	213.3	212.1	206.7	207.1	204.8
PDPA-NO_2	213.5	220.1	210.9	206.8	212.9	203.9
	219.7	219.2	218.3	213.0	212.2	211.2
PDPA: 5-methyl-2-phenyl-4-(2-phenylhydrazono)-2,4-dihydro-3H-pyrazol-3-one.						

In general, our results show that the stronger the EDG power is, the more basic the center is, while the stronger the EWG power is, the less basic the center is (Grabowski 2001; Safi and Frenking 2013; Safi and Omar 2014). For the N1 atom, results in Table 1 demonstrate that the maximum PA values of ~229 and ~ 227 kcal/mol correspond to -NH_2 and -CH_3 derivatives, respectively. These results can be attributed to the higher ability of the lone-pair electrons on the N atom of the NH_2 group, as well as the inductive effect of the CH_3 group, leading to an increase the electron density of the N1 atom, and consequently increasing the tendency of the N1 atom to interact with the incoming proton. On the other hand, the lowest PA value of 213.5 kcal/mol belongs to -CN and -NO_2 derivatives, indicating that substitution of electron withdrawing groups decreases the electron density on the N1 atom, and consequently, decreases the propensity of the interaction of the N1 atom with the proton. A similar interpretation can also be used for GB results. These results can be confirmed by investigating the NBO results. Data in Table SM2 show that the maximum occupancies of the neutral and protonated N1 atom, ($LP(1)_{N1}$), of 1.9456 and 1.7682 a.u., respectively. Whereas the minimum occupancies for the same atom are 1.9386 and 1.6336 a.u., respectively. Therefore, the intrinsic basicity of N1 atoms of the investigated derivatives can be arranged as follows: PDPA-NH_2 > PDPA-CH_3 > PDPA-H > PDPA-Cl > PDPA-F > PDPA-CHO > PDPA -CN ≈ PDPA-NO_2.

For the N3 atom, an irregular decrease was observed in the PA and GB values of PDPA-NH_2 derivative compared to the parent molecule, see Table 1. In contrast, an unexpected increase in the PA and GB values of PDPA-CHO and PDPA-NO_2 derivatives compared to the parent molecule, which might be explained in terms of the formation of a weak IMHB between the proton and the oxygen atom of both -CHO and -NO_2 groups, resulting in reducing the potential of the positive charge of the incoming proton. For N4, the trends of PA and GB values are almost similar to N1, except for the PDPA-CHO molecule, which is 6.3 kcal/mol higher than that of PDPA-H. It is found that the PA of the PDPA-CHO derivative is higher than that of the parent molecule by 6.3 kcal/mol. For both N3 and N4 atoms, the presence of the phenyl group, which is directly bonded to the azo-dye group, has a crucial role in decreasing the basicity due to the delocalization effect.

The geometries of the neutral and protonated (at N1) forms of some investigated derivatives, including PDPA-H, PDPA-NH, PDPA-CHO, and PDPA-NO_2, have been shown in Fig. 1, while the other derivatives have been shown in Fig. SM2 of the supplementary materials. Full geometries of the protonated forms, at N2 and N3 atoms, are available from authors upon request.

A general inspection of the results obtained shows that the bond lengths and bond angles of the investigated derivatives exhibit the expected variation upon protonation. It is found that the most effective changes are located in the bond lengths and the bond angles neighboring the protonated nitrogen atom, while slight variations are observed for other bonds. The C_5=N_1 and N_1-N_2 bond distances lengthen with averages of, correspondingly, 0.050 and 0.003 Å, while the $\angle N_2N_1C_3$ angle increases with an average of 3.3°. In addition, the phenyl group attached to the pyrazole ring is twisted out of plane. It is also found that the average bond distances of $N_i \ldots H^+$ $(i = 1,3, \text{and} 4)$, are 1.014, 1.027, and 1.023 Å, respectively, which agree with the PA results. This signifies that the interaction between the N1 atom and the incoming proton is the strongest one.

3.2 Analysis of single water-PDPA interactions

Frontier orbital theory (FOT) affirms that the most reactive molecular orbitals (MO) in the molecule are the highest occupied and the lowest unoccupied molecular orbitals (HOMO and LUMO). The

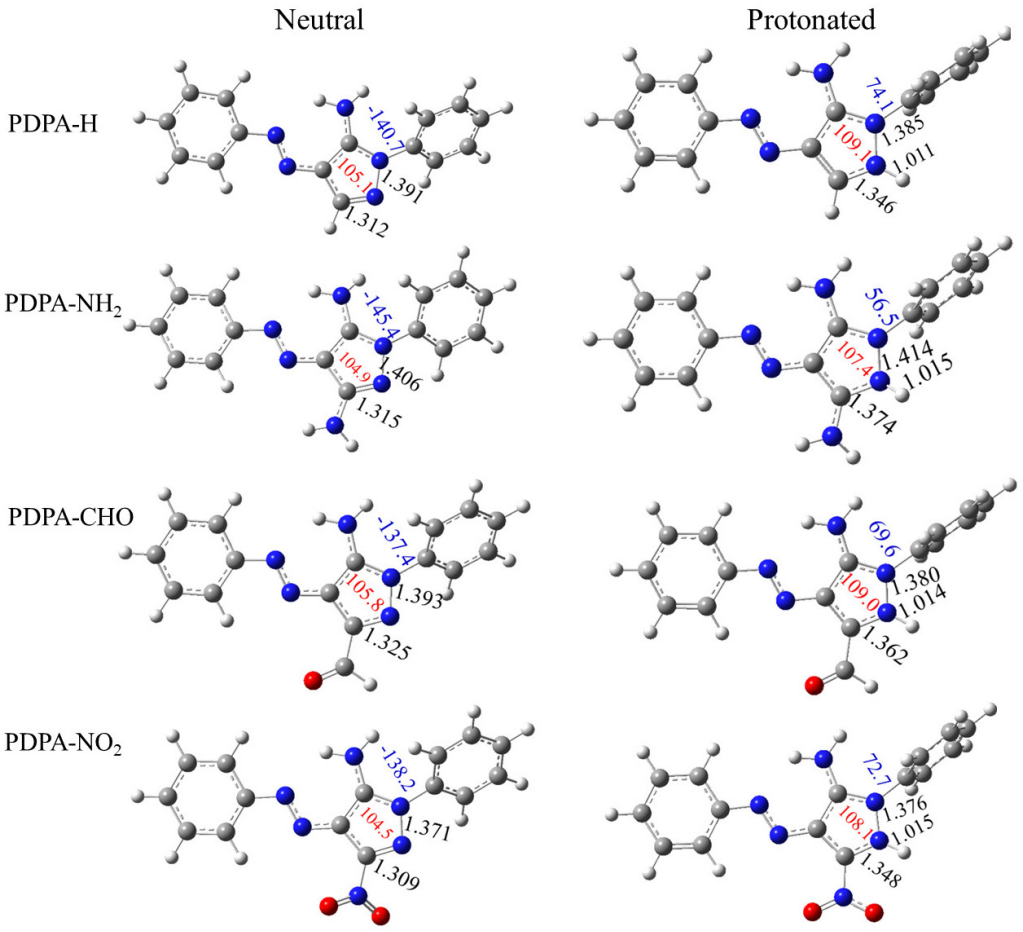

Fig. 1. Optimized structure of neutral and protonated forms at N1 atom of PDPA-H, PDPA-NH_2, PDPA-CHO and PDPA-NO_2 derivatives. Bond lengths, C5-N1, N1 = N2 and N1-H^+ in Å (black color), the ∠N2N1C5 bond angle in (°) (in red color) and the dihedral angle, $\varphi_{C5N1N2C6}$ in (°) are shown in blue color.

energy gaps of the individual water and PDPA derivatives (ΔE) and those of water-PDPA interactions (ΔE_1 and ΔE_2) can be calculated using the following expressions Eq. (2).

$$\left\{\begin{array}{l} E = \left|E_{HOMO} - E_{LUMO}\right| \\ \Delta E_1 = \left|E_{HOMO}^{H_2O} - E_{LUMO}^{PDPA}\right| \\ \Delta E_2 = \left|E_{HOMO}^{PDPA} - E_{LUMO}^{H_2O}\right| \end{array}\right\} \quad (2)$$

The corresponding E_{HOMO} and E_{LUMO} and HOMO-LUMO energy gaps (ΔE, ΔE1 and ΔE_2) have been displayed in Table 2.

A larger E_{HOMO} value is known to accelerate the atom's tendency to donate electrons, while a lower E_{LUMO} increases the atom's propensity to accept electrons. Examination of Table 2 indicates that the PDPA-NH_2 derivative has the highest capability to donate electrons to water molecules, while the PDPA-NO_2 derivative has the lowest. Contrarily, the PDPA-NO_2 derivative has the maximum ability to accept electrons, while PDPA-NH_2 has the minimum. These results clearly indicate that as the substitution of EDG increases, the electron density of the lone pair of electrons on N1 increases, consequently increasing its ability to donate electrons to the LUMO of the water molecule. In contrast, the substitution of EWG decreases the electron density on N1 therefore increasing it's ability to accept electrons from water molecules. It is also found that the studied PDPA derivatives are characterized by small energy gaps, which lie in the range of 3.565-3.732 eV, signifying that they are chemically reactive and kinetically unstable.

Insight of the above findings, the question to be addressed is whether the electron's flow is more favorable. The results in Table 2 clearly indicate that $\Delta E_2 < \Delta E_1$, signifying that the electrons flow can take place from the HOMO of PDPA derivatives to the LUMO of water. This means that the interaction between the H_2O and PDPA molecules might have occurred by the interaction of the lone pair of electrons of the N1 atom of PDPA derivatives and the hydrogen water molecule. It is also found that as the power of EDG increases, the N1…H interaction power increases. Contrarily, EWG substitution decreases the strength of the N1…H interaction. Therefore, it can be predicted that the strength of N1…H interaction can be arranged as follows: PDPA -NH_2 > PDPA -CH_3 > PDPA -H > PDPA -Cl > PDPA -F > PDPA -CHO > PDPA -CN > PDPA -NO_2.

The solvent effect was explicitly performed by the interaction of PDPA derivatives with single water molecules at the N1 atom through the formation of IMHB. Fig. 2 shows the geometrical structures of the PDPA-water complexes. The first inspection of Fig. 2 shows that the bond distance of N_1…H in the PDPA-water complexes lies between 1.926 – 2.379 Å. Among the investigated complexes, the longest N_1…H bond of 2.379 Å was found for the PDPA-NO_2.H_2O complex, which is attributed to the possible formation of another IMHB with 2.290 Å between the hydrogen water molecule and the oxygen NO_2 group. On the other hand, the shortest IMHB of 1.953 Å, corresponds to the PDPA-NH_2.H_2O complex.

Table 2.
Frontier orbital energies of water and PDPA derivatives (E_{HOMO} and E_{LUMO} in eV), and the energy gaps values (ΔE, ΔE_1 and ΔE_2 in eV) of PDPA derivatives and water molecule.

Derivative	E_{HOMO}	E_{LUMO}	ΔE	ΔE_1	ΔE_2
H_2O	-8.788	-0.634	8.155	-	-
PDPA-H	-5.836	-2.172	3.664	6.616	5.202
PDPA -CH_3	-5.766	-2.127	3.639	6.661	5.132
PDPA -NH_2	-5.727	-2.114	3.613	6.674	5.093
PDPA -Cl	-6.028	-2.321	3.707	6.467	5.394
PDPA -F	-6.053	-2.321	3.732	6.467	5.419
PDPA -CHO	-6.063	-2.446	3.617	6.342	5.429
PDPA -CN	-6.253	-2.578	3.675	6.210	5.619
PDPA -NO_2	-6.323	-2.758	3.565	6.030	5.689
Average	-6.006	-2.355	3.652	6.434	5.372

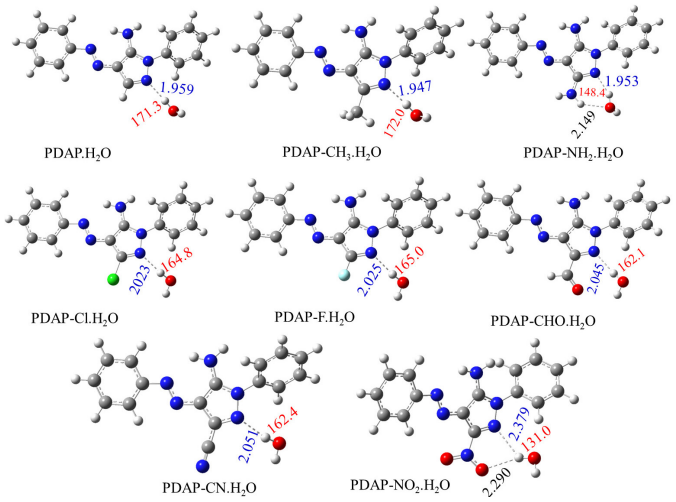

Fig. 2. Optimized structure of PDPA-H_2O complexes and its derivatives as obtained using B3LY{/6-311++G(d,p) level of theory. The intermolecular hydrogen bond length and bond angle between PDPA and water N_3…H as shown in blue and red colors, respectively. Units are in Å for N_3…H bond length and in (°) for $\angle N_1HO$ bond angles.

In general, our results indicate that as the power of EWGs increases, the length of the IMHB decreases, which can be explained by the increase in electron density at the N1 atom and vice versa. It is also found that as the strength of EDG increases, the hydrogen bond angle, $\angle N_1HO$, increases. Contrary, as the strength of EWG increases, the $\angle N_1HO$ decreases, see Fig. 2.

The intermolecular interactions between the water molecule and the PDPA derivatives can be represented by plotting the scatter plot of $\delta\, g^{inter/intra}$ *(a.u.) vs. sign*$(\lambda_2)\rho$ *(a.u.)* and the corresponding RGD maps, see Fig. 3 and Fig. SM3 of the supplementary materials. As seen in Figs. 3 and SM3, the intermolecular region has been represented by red dots, while the intramolecular interactions have been represented by black dots. The density of the red region reflects the strength of the intermolecular interactions between water molecules and PDPA derivatives. The density of the red dot is directly proportional to the intermolecular interaction. It is obvious from Fig. 3 that minimum intermolecular interaction corresponds to the PDPA-NO_2.H_2O complex, which the maximum one belongs to, correspondingly, PDPA-NH_2.H_2O complex.

The above results have been confirmed by the estimation of the interaction energy (E_{int}) of the $PDHP + H_2O \rightleftarrows PDHP.H_2O$ reaction using the following expression:

$$E_{int} = E_{complex} - (E_{PDAP} - E_{H_2O}) \quad (3)$$

Here, $E_{complex}$, E_{PDPA} and E_{H2O} are the single point energies with the corrected ZPE of PDPA-water complexes, PDPA derivatives and water molecule, respectively. The corresponding E_{int} values have been listed in Table 3. The corresponding energies, ZPE and Thermal corrections have also been displayed in Table SM1.

Our results show that the average E_{int} value is -5.0 kcal/mol, which belongs to moderate IMHB. The maximum E_{int} value of -6.6 kcal/mol corresponds to PDPA-NH_2.H_2O, while the minimum one of -4.2 kcal/mol belongs to the PDPA-CN.H_2O complex, illustrating the significant role of the nature of substituted groups in the strengthening or the weakening the IMHB. Furthermore, a second-order NBO perturbation analysis clearly depicts the interaction between the lone pairs of electrons on the N1 atom of PDPA derivatives, $LP(1)_{N1}$ nonbonding orbital, and the σ^*_{H-O} antibonding orbitals of water molecule ($LP(1)_{N1} \rightarrow \sigma^*_{H-O}$), resultsing in a stabilization energy (E^{CT}). This E^{CT} enhances system stabilization by intermolecular charge transfer. According to Table 3, the E^{CT} value ranges from 0.62 to 9.7 kcal/mol, ensuring a moderate strength IMHB. The existence of an additional electron transfer is also observed in the case of PDPA-NH_2.H_2O and PDPA-NO_2.H_2O complexes. The extra stabilization of the PDPA-NH_2.H_2O complex

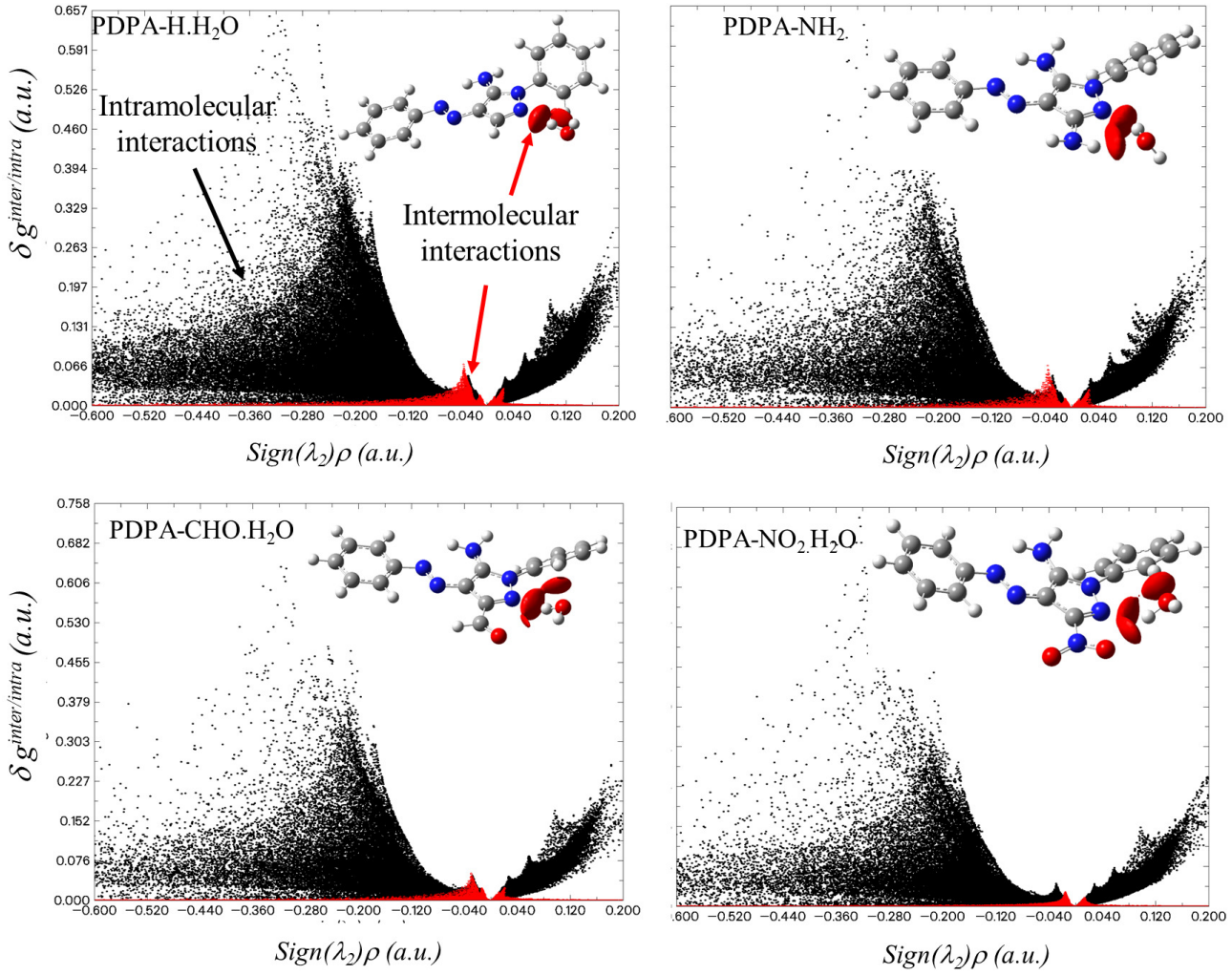

Fig. 3. Scatter plots of $\delta g^{inter/intra}$ *(a.u.) vs. Sign*(λ_2)ρ *(a.u)* of some PDPA-water complexes. The corresponding RGD maps are superimposed at the top right of each panel. The red dots correspond to the intermolecular interactions, while the black dots correspond to the intramolecular interactions. The corresponding plots of the other species have been shown in Figure SM3 of the supplementary materials

Table 3.
Interaction energy, E_{int}, electron transfer energy, E^{CT}, which *corresponds to* the $LP(1)_{N1} \rightarrow \sigma^*_{H-O}$;), and IMHB energy, E_{HB}, *(in kcal/mol),* as well as the topological parameters computed at the BCP (3, −1) of the IMHB, including $\rho_{BCP}(r)$, $\nabla^2\rho(r)$, (G(*r*), H(*r*), and V(*r*), and the bond order (BO) of the PDPA-water complexes. E^{CT} values between brackets correspond to the $(LP(2)O) \rightarrow \sigma^*_{N-H}$ and $(LP(2)O) \rightarrow \sigma^*_{H-O}$ interactions, respectively. E_{int}, E^{CT} and E_{HB} are in kcal/mol, topological parameters are in a.u., and BO is unitless.

Species	E_{int}	E^{CT}	$\rho_{BCP}(r)$	$\nabla^2_{\rho BCP}(r)$	[b] G(r)	H(r)	V(r)	G(r)	BO	E_{HB}
PDPA-H.H_2O	-4.8	9.0	0.0275	0.0867	0.0205	-0.0012	-0.0193	0.0205	0.94	6.1
PDPA-CH_3.H_2O	-5.0	9.7	0.0285	0.0883	0.0212	-0.0009	-0.0202	0.0212	0.96	6.4
PDPA-NH_2.H_2O	-6.6	9.5 (3.4)	0.0295	0.0924	0.0225	-0.0006	-0.0219	0.0225	0.97	6.9
PDPA -Cl.H_2O	-4.5	6.4	0.0237	0.0775	0.0175	-0.0019	-0.0156	0.0175	0.89	4.9
PDPA -F.H_2O	-4.4	6.5	0.0235	0.0772	0.0173	-0.002	-0.0153	0.0173	0.89	4.8
PDPA-CHO.H_2O	-4.7	5.5	0.0223	0.0753	0.0167	-0.0022	-0.0145	0.0167	0.87	4.5
PDPA-CN.H_2O	-4.2	5.5	0.0223	0.074	0.0164	-0.0021	-0.0143	0.0164	0.87	4.5
PDPA-NO_2.H_2O	-5.5	0.6 (1.6)	0.011	0.0395	0.0082	-0.0017	-0.0065	0.0082	0.79	2.0
Average values	-5.0	6.7	0.02354	0.0764	0.89750	0.01754	-0.0016	-0.0160	0.01754	5.0

is due to the $((LP(2)O) \rightarrow \sigma^*_{N-H})$ interaction, which is associated with an E^{CT} of 3.4 kcal/mol. On the other hand, the interaction between the nonbonding orbitals of oxygen nitro group with antibonding orbitals of the O-H of water molecule $((LP(2)O) \rightarrow \sigma^*_{H-O})$, which is associated with E^{CT} of 1.6 kcal/mol, destabilizes the PDPA-NO_2.H_2O complexes.

Additional understanding of the nature of the IMHB in PDPA-water complexes can be obtained by analyzing the AIM results of Bader's theory (Bader 1991). Analysis of the BCP's properties was usually utilized to estimate the hydrogen bond strength (Nguyen and Chandra 1998; Lamsabhi 2008; Safi 2016). The most relevant results topological properties, including the electron charge, $\rho_{BCP}(r)$, computed at the BCP

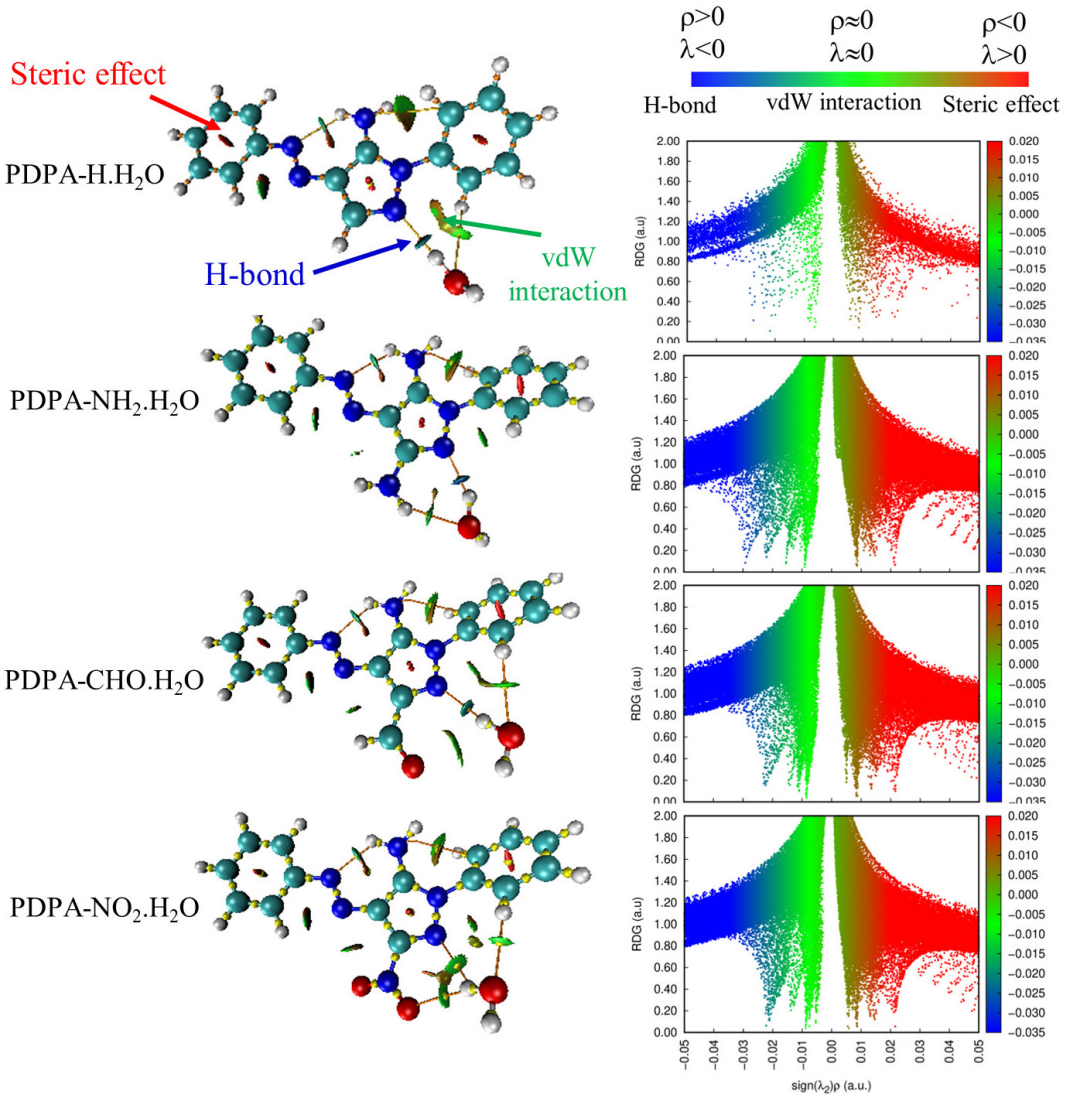

Fig. 4. RDG maps (left) and Scatter plots of RDG (a.u.) versus Sign(λ_2)ρ (a.u) (right) of some PDPA-water complexes, including PDPA-H.H_2O, PDPA-NH_2.H_2O, PDPA-CHO.H_2O, and PDPA-NO_2.H_2O. Note: Molecular graphs based on QTAIM are superimposed (left images, orange points, and yellow lines).

(3, −1) for the IMHB and its related parameters, including Laplacian ($\nabla^2\rho(r)$), Lagrangian and Hamiltonian kinetic energies (G(*r*) and H(*r*), and the potential electron density (V(*r*), have been displayed in Table 3. The corresponding molecular graphs have been shown in Fig. 3. It was discovered that $\rho_{BCP}(r)$ and $\nabla^2_{\rho_{BCP}}(r)$ values fall within the hydrogen bond range with averages of 0.0253 and 0.0816 a.u., respectively, indicating that the investigated IMHB belongs to medium interaction (Nguyen and Chandra 1998; Lamsabhi 2008). The largest $\rho_{BCP}(r)$ (0.0924 a.u.) was reported for the PDPA-NH_2.H_2O complex, while the smallest value (0.0395 a.u.) was for the PDPA-NO_2.H_2O complex. Our results in Table 3 strongly affirm that substitution of the EDGs increases the $\rho_{BCP}(r)$ and its related topological parameters, while substitution of EWGs decreases the $\rho_{BCP}(r)$ and its related topological parameters. Furthermore, the IMHB energy and its bond order (BO) were evaluated as E_{HB} = -*V*(*r*)/2) (Espinosa *et al.*, 1998), and *BO*= $|V(r)|/G(r)$ and their results have been displayed in Table 3. Our results show that the average value of the BO is 0.91, with maximum and minimum BO values corresponding to PDPA-NH_2.H_2O and PDPA-NO_2.H_2O complexes, respectively. It is also found that E_{HB} values are ranged from 1.6 to 6.9 kcal/mol, which confirm the results of E_{int} and E^{CT}, in agreement with similar systems (Nguyen and Chandra 1998; Lamsabhi 2008; Safi 2016).

The NCI's plot is useful in illustrating the correlation between strong directional attractions with the localized atom-atom contacts and the molecular division having weak interactions. The color-filled RDG isosurfaces and the scatter plots of the Hessian of the electron density, *Sign*(λ_2)ρ, for some PDPA-water complexes have been shown in Fig. 4, while the other plots have been shown in Fig. SM4 of the supplementary materials. Examination of RDG isosurfaces indicate three different regions, which correspond to (i) weak interaction forces (green color) that occur between the atoms in the molecule, (ii) strong field interactions (red arrow) belong to steric effect of the aromatic rings and (iii) hydrogen bond interactions (blue color). A close examination of the 3D-Isosurface of color scaling of weak interactions diagram (NIC, Fig. 4 (right)) indicates that the interactions between LP(1)N_1 (proton acceptor) and the proton donor (hydrogen water molecule) are stronger in case of NH_2 and CH_3 derivatives compared to the others. Except for the PDPA-NO_2.H_2O complex, the presence of another IMHB field is indicated by the presence of blue circle (assigned by a blue arrow). A weak IMHB field was also observed between the oxygen nitro group (-NO_2 derivative) and the hydrogen water in case of PDPA-NO_2. Also, another IMHB region was observed between the oxygen water molecule and the amino hydrogen atom in the case of PPDPA-NH_2.H2O complex. These results agreed with NBO results as discussed above.

4. Conclusions

Several derivatives of polyfunctional azo dye pyrazole-based (PDPA) were computationally studied for explicit solvent effects. The protonation sites were identified using two strategies based on DFT and *pKa* calculations. Results reveal that *pKa*, as a rapid calculation, is useful for identifying the protonation sites with some limitations, especially for -F and -NO_2 groups. On the other hand, DFT/ B3LYP(6-311++G(3df,2p) predicts the appropriate site for protonation based on PA values. The PA and GB values suggest that PDPA and its derivatives are potent and basic, and the nature of the substituted group has a great impact on the intrinsic basicity. The stronger the EDGs, the higher the PA and GB values, while the stronger the EWGs, the lower the PA and GB values. The PDHP-water interaction shows a moderate-strength intermolecular hydrogen bond between the nitrogen atom and the water molecule. Interaction energies, NBO analysis, and topological properties within the framework of the QTAIM concluded that the PDPA-NH_2.H_2O complex has the strongest IMHB, while the PDPA-CN. H_2O and PDPA-NO_2.H_2O complexes have the weakest one. Based on the results obtained in this article, the research can be extended to study the non-covalent interactions between the between the PDPA and its derivatives with different solvents, including protic and aprotic solvents.

CRediT authorship contribution statement

Nuha Wazzan: Methodology, Investigation, Resources, Writing - Review & Editing, Project administration; **Zaki Safi:** Conceptualization, Methodology, Validation, Formal analysis, Investigation, Data Curation, Writing - Review & Editing, Visualization.

Declaration of competing interest

The authors declare that they have no known competing financial interests or personal relationships that could have appeared to influence the work reported in this paper.

Declaration of Generative AI and AI-assisted technologies in the writing process

The authors confirm that there was no use of Artificial Intelligence (AI)-Assisted Technology for assisting in the writing or editing of the manuscript and no images were manipulated using AI.

Acknowledgments

Authors gratefully acknowledge King Abdulaziz University's High-Performance Computing Centre (Aziz Supercomputer) (http://hpc.kau.edu.sa) for assisting with the calculations for the work of this paper.

Supplementary material

Supplementary data to this article can be found online at https://dx.doi.org/10.25259/JKSUS_259_2024.

References

Bader, R.F., 1991. A quantum theory of molecular structure and its applications. Chemical Reviews, 91(5), pp. 893-928.

Bani-Yaseen, A.D., 2017. Computational molecular perspectives on the interaction of propranolol with β-cyclodextrin in solution: Towards the drug-receptor mechanism of interaction. J. Mol. Liq. 227, 280-290. https://doi.org/10.1016/j.molliq.2016.12.023

Bayoumy, A.M., Refaat, A., Yahia, I.S., Zahran, H.Y., Elhaes, H., Ibrahim, M.A., Shkir, M., 2020. Functionalization of graphene quantum dots (GQDs) with chitosan biopolymer for biophysical applications. Opt Quant Electron 52. https://doi.org/10.1007/s11082-019-2134-z

Becke, A.D., 1996. Density-functional thermochemistry. IV. A new dynamical correlation functional and implications for exact-exchange mixing. J. Chem. Phys. 104, 1040-1046.

Blake, R.S., Monks, P.S., Ellis, A.M., 2009. Proton-transfer reaction mass spectrometry. Chem. Rev. 109, 861-896. https://doi.org/10.1021/cr800364q

Cerezo, J., Avila Ferrer, F.J., Prampolini, G., Santoro, F., 2015. Modeling solvent broadening on the vibronic spectra of a series of coumarin dyes From implicit to explicit solvent models. J. Chem. Theory Comput. 11, 5810-5825. https://doi.org/10.1021/acs.jctc.5b00870

Cherinka, B., Andrews, B.H., Sánchez-Gallego, J.é, Brownstein, J., Argudo-Fernández, M.ía, Blanton, M., Bundy, K., Jones, A., Masters, K., Law, D.R., Rowlands, K., Weijmans, A.-M., Westfall, K., Yan, R., 2019. Marvin: A tool kit for streamlined access and visualization of the SDSS-IV maNGA data set. AJ 158, 74. https://doi.org/10.3847/1538-3881/ab2634

Comez, L., Paolantoni, M., Sassi, P., Corezzi, S., Morresi, A., Fioretto, D., 2016. Molecular properties of aqueous solutions: A focus on the collective dynamics of hydration water. Soft Matter 12, 5501-5514. https://doi.org/10.1039/c5sm03119b

Correia, V.M., Stephenson, T., Judd, S.J., 1994. Characterisation of textile wastewaters-a review. Environ. Technol. 15, 917-929.

Deneva, V., Lyčka, A., Hristova, S., Crochet, A., Fromm, K.M., Antonov, L., 2019. Tautomerism in azo dyes: Border cases of azo and hydrazo tautomers as possible NMR reference compounds. Dyes Pigm. 165, 157-163. https://doi.org/10.1016/j.dyepig.2019.02.015

Dennington, R., Keith, T., Millam, J., 2016. GaussView, Version 6.1 GaussView, Version 61. Semichem Inc, Shawnee Mission

Dixon, D., Lias, S., 1987. Molecular structure and energetics. In: Liebman, JF, Greenberg, A., editors. Physical Measurements, VCH, Deereld Beach, FL; p. 269.

El-Sayed, N.M., Elhaes, H., Ibrahim, A., Ibrahim, M.A., 2024. Investigating the electronic properties of edge glycine/biopolymer/graphene quantum dots. Sci. Rep. 14, 21973. https://doi.org/10.1038/s41598-024-71655-1

Espinosa, E., Lecomte, C., Ghermani, N., Devémy, J., Rohmer, M., Bénard, M., Molins, E., 1996. Hydrogen bonds: first quantitative agreement between electrostatic potential calculations from experimental X−(X+ N) and theoretical ab initio SCF models. J. Am. Chem. Soc. 118, 2501-2502.

Espinosa, E., Molins, E., Lecomte, C., 1998. Hydrogen bond strengths revealed by topological analyses of experimentally observed electron densities. Chem. Phys. Lett. 285, 170-173. https://doi.org/10.1016/s0009-2614(98)00036-0

Gaussian09, R.A., 2009. 1, mj frisch, gw trucks, hb schlegel, ge scuseria, ma robb, jr cheeseman, g. Scalmani, v. Barone, b. Mennucci, ga petersson *et al.*, gaussian. Inc., Wallingford CT 121, 150-166.

Geng, J., Dai, Y., Qian, H.-F., Wang, N., Huang, W., 2015. 2-amino-4-chloro-5-formylthiophene-3-carbonitrile derived azo dyes. Dyes Pigm. 117, 133-140. https://doi.org/10.1016/j.dyepig.2015.02.010

Grabowski, S., 2001. An estimation of strength of intramolecular hydrogen bonds—ab initio and AIM studies. J. Mol. Struct. 562, 137-143.

Humphrey, W., Dalke, A., Schulten, K., 1996. VMD: Visual molecular dynamics. J. Mol. Graph. 14, 33-38. https://doi.org/10.1016/0263-7855(96)00018-5

Jolly, W.L., 1991. Modern inorganic chemistry.

Kelley, T.W.C. 2004-2021. gnuplot 5.5 An Interactive Plotting Program. [accessed 2024 Oct 01]. Available from: http://sourceforge.net/projects/gnuplot.

Lamsabhi, A.M., 2008. Specific hydration effects on oxo-thio triazepine derivatives. J. Phys. Chem. A 112, 1791-1797. https://doi.org/10.1021/jp709960g

Lu, T., Chen, F., 2012. Multiwfn: A multifunctional wavefunction analyzer. J. Comput. Chem. 33, 580-592. https://doi.org/10.1002/jcc.22885

Meghwal, K., Kumawat, S., Ameta, C., Jangid, N.K., 2020. Effect of dyes on water chemistry, soil quality, and biological properties of water. Impact of textile dyes on public health and the environment, IGI Global Scientific Publishing: 90-114.

Tho Nguyen, M., Chandra, A.K., Zeegers-Huyskens, T., 1998. Protonation and deprotonation energies of uracil implications for the uracil–water complex. Faraday Trans. 94, 1277-1280. https://doi.org/10.1039/a708804c

Osman, O.I., 2017. DFT study of the structure, reactivity, natural bond orbital and hyperpolarizability of thiazole azo dyes. Int. J. Mol. Sci. 18, 239. https://doi.org/10.3390/ijms18020239

Rebber, B.L., Halfacre, J.A., Beran, K.A., Beller, N.R., Gomez, M., Bashir, S., Giannakopulos, A.E., Derrick, P.J., 2006. Theoretical investigation of the proton affinity and gas-phase basicity of neutral x,y-dihydroxybenzoic acid and its derivatives. Eur J Mass Spectrom (Chichester) 12, 385-396. https://doi.org/10.1255/ejms.823

Reed, A.E., Curtiss, L.A., Weinhold, F., 1988. Intermolecular interactions from a natural bond orbital, donor-acceptor viewpoint. Chem. Rev. 88, 899-926. https://doi.org/10.1021/cr00088a005

S. Grimme, J.A., S. Ehrlich, H. Krieg, 2010. A consistent and accurate ab initio parametrization of density functional dispersion correction (DFT-D). J. Chemical. Physics. review. B 132, 154104.

Safi, Z., Lamsabhi, A.M., 2007. Gas-phase reactivity of 2,7-dimethyl-[1,2,4]-triazepine thio derivatives toward cu+Cation: A DFT study. J. Phys. Chem. A 111, 2213-2219. https://doi.org/10.1021/jp068642h

Safi, Z.S., 2016. A theoretical study on the structure of thiazolidine-2,4-dione and its 5-substituted derivatives in the gas phase Implications for the thiazolidine-2,4-dione -water complex. Arab. J. Chem. 9, 616-625. https://doi.org/10.1016/j.arabjc.2015.03.016

Safi, Z.S., Frenking, G., 2013. Protonation of 5-methylhydantoin and its thio derivatives in the gas phase: A theoretical study. Int J of Quantum Chemistry 113, 908-915. https://doi.org/10.1002/qua.24017

Safi, Z.S., Omar, S., 2014. Proton affinity and molecular basicity of m-and p-substituted benzamides in gas phase and in solution: a theoretical study. Chem. Phys. Lett. 610, 321-330.

Safi, Z.S., Wazzan, N., 2021. Benchmark calculations of proton affinity and gas-phase basicity using multilevel (G4 and G3B3), B3LYP and MP2 computational methods

of para-substituted benzaldehyde compounds. J. Comput. Chem. 42, 1106-1117. https://doi.org/10.1002/jcc.26538

Tabrizchi, M., Shooshtari, S., 2003. Proton affinity measurements using ion mobility spectrometry. J. Chem. Thermodyn. 35, 863-870. https://doi.org/10.1016/s0021-9614(02)00316-6

Valadbeigi, Y., Farrokhpour, H., 2013. DFT, CBS-Q, W1BD and G4MP2 calculation of the proton and electron affinities, gas phase basicities and ionization energies of saturated and unsaturated carboxylic acids (C1–C4). Int. J. Quantum Chem. 113, 1717-1721.

Safi, Z.S., Wazzan, N., 2021. Benchmark calculations of proton affinity and gas-phase basicity using multilevel (G4 and G3B3), B3LYP and MP2 computational methods of para-substituted benzaldehyde compounds. J. Comput. Chem. 42, 1106-1117. https://doi.org/10.1002/jcc.26538

Zhao, J., Zhang, R., 2004. Proton transfer reaction rate constants between hydronium ion (H3O+) and volatile organic compounds. Atmos. Environ. 38, 2177-2185. https://doi.org/10.1016/j.atmosenv.2004.01.019

Zollinger, H., 2003. Color chemistry: syntheses, properties, and applications of organic dyes and pigments, John Wiley & Sons.